T cells induce interleukin 10-producing, contact-independent type 1-like regulatory T cells. *J Exp Med* 2002; 196: 247–53.

33 Jonuleit H, Schmitt E, Kakirman H, Stassen M, Knop J, Enk AH. Infectious tolerance: human CD25(+) regulatory T cells convey suppressor activity to conventional CD4(+) T helper cells. *J Exp Med* 2002; 196: 255–60.

34 Foussat A, Cottrez F, Brun V, Fournier N, Breittmayer JP, Groux H. A comparative study between T regulatory type 1 and CD4+CD25+ T cells in the control of inflammation. *J Immunol* 2003; 171: 5018–26.

35 Simark-Mattsson C, Dahlgren U, Roos K. CD4+CD25+ T lymphocytes in human tonsils suppress the proliferation of CD4+CD25– tonsil cells. *Scand J Immunol* 2002; 55: 606–11.

36 Takahashi T, Kuniyasu Y, Toda M *et al.* Immunologic self-tolerance maintained by CD25+CD4+ naturally anergic and suppressive T cells: induction of autoimmune disease by breaking their anergic/suppressive state. *Int Immunol* 1998; 10: 1969–80.

37 Mieza MA, Itoh T, Cui JQ *et al.* Selective reduction of V alpha 14+ NK T cells associated with disease development in autoimmune-prone mice. *J Immunol* 1996; 156: 4035–40.

38 Wilson MT, Van Kaer L. Natural killer T cells as targets for therapeutic intervention in autoimmune diseases. *Curr Pharm Des* 2003; 9: 201–20.

39 Kojo S, Adachi Y, Keino H, Taniguchi M, Sumida T. Dysfunction of T cell receptor AV24AJ18+, BV11+ double-negative regulatory natural killer T cells in autoimmune diseases. *Arthritis Rheum* 2001; 44: 1127–38.

Chapter 30
The Protective Effect of Taurine Against Hepatic Damage in a Model of Liver Disease and Hepatic Stellate Cells

Teruo Miyazaki, Bernard Bouscarel, Tadashi Ikegami, Akira Honda, and Yasushi Matsuzaki

Abstract Taurine plays a protective role against free radicals and toxins in various cells and tissues. However, the effect of taurine on hepatic injury and fibrosis developed by activated hepatic stellate cells (HSC) and myofibroblast-like cells is not fully understood. We investigated the effects of taurine on the hepatic fibrogenesis and damage in rats and isolated HSC. Rats were divided into a normal and two CCl_4-induced liver damage (LD) groups, one untreated and the other maintained for 5 weeks on a 2% taurine diet. The HSC isolated from a normal rat were cultured either for a day only or for an additional 3–6 days with ~50 mM taurine. LD rats maintained on the taurine diet were resistant to CCl_4-induced loss of taurine from the liver. The liver of the LD rats were also protected against histological damage, fibrosis, significant reductions in oxidative stress markers (LPO and 8-OHdG) and hepatic fibrogenic factors (TGF–β_1 mRNA, hydroxyproline, α-SMA). Proliferation, oxidative stress, and fibrogenesis were significantly inhibited in HSC by treatment with taurine. Thus, supplementation with taurine should be considered as a therapeutic approach to lessen the severity of oxidative stress-induced liver injury and hepatic fibrosis.

Abbreviations *HSC*, hepatic stellate cells; *CCl_4*, carbon tetrachloride, *LPO*, lipid hydroperoxide; *TGF–β_1*, transforming growth factor–β_1; *α-SMA*, α-smooth muscle actin protein

T. Miyazaki (✉)
The George Washington University, District of Columbia, USA

J. Azuma et al. (eds.), *Taurine 7*, Advances in Experimental Medicine and Biology 643,
DOI 10.1007/978-0-387-75681-3_30, © Springer Science+Business Media, LLC 2009

30.1 Introduction

Taurine, 2-amino ethylsulfonic acid, is the most abundant amino acid in mammalian tissues, including heart (Awapara 1956), skeletal muscle (Jacobsen and Swimth 1968), nerve, brain, and liver (Jacobsen and Swimth 1968; Huxtable 1980). The plasma and intracellular concentration of taurine are considerably higher than those of other amino acids; plasma: 200~250μM), heart: 25~30mM (Timbrell et al.1995), lung: 11~27mM (Timbrell et al. 1995), neutrophils: 50~100mM (Fukuda et al. 1982; Green 1991), retina: 50~ 70mM (Sturman 1993). The high intracellular levels of taurine are maintained by active uptake and endogenous synthesis ,mainly in the liver where taurine is an endproduct of sulfur amino acid catabolism (Hosokawa et al. 1990; Kaisaki et al. 1995; Reymond et al. 1996; Tappaz et al. 1999). The biosynthesis of taurine in the liver is limited, particularly in the case of liver disease, where the biosynthetic ability might be reduced. Therefore, exogenous uptake via the diet is largely responsible for maintaining the high intracellular concentration of taurine that account for its many physiological and pharmacological roles, including cellular plasma membrane stabilization (Pasantes et al. 1985), osmoregulation (Nieminen et al. 1988), neuromodulation and neurotransmission (Davison and Kaczmarec 1971; Kuriyama 1980; Kanner and Nurit 1994), anti-oxidation (Nakashima et al. 1990; Waterfield et al. 1993a, b; Timbrell et al. 1995), detoxification (Huxtable 1992) and conjugation to bile acids in the liver (Sjovall 1959; Danielsson 1963).

We have demonstrated the effects of taurine on oxidative stress induced by exercise and/or by hepatotoxin in rats. In exercised rats, oral taurine administration reduced oxidative stress (lipid peroxidation, oxidized glutathione) and diminished the decrease in taurine content of skeletal muscle (Miyazaki et al. 2004a). Hepatic taurine concentration was significantly decreased in liver disease mediated by a free radical inducer CCl_4 (Miyazaki et al. 2004b). Previous studies have shown that taurine treatment inhibits hepatic damage induced by CCl_4-mediated oxidative stress (Vohra and Hui 2001; Dinçcer et al. 2002) and thioacetamide-mediated toxicity (Balkan et al. 2001). Indeed, the anti-oxidant activity of taurine has been reported in chick heart (Azuma et al. 1987), hamster lung (Wang et al. 1991; Gordon et al. 1992), and the rat central nervous system (Vohra and Hui 2001), as well as in human lymphoblastoid cells (Pasantes et al. 1984), neutrophils (Wright et al. 1985), and blood cells in culture (Koyama et al. 1992). Therefore, these results show that taurine serves as an anti-oxidant to prevent liver disease.

Oxidative stress and cytokine tranforming growth factor-beta$_1$ (TGF$-\beta_1$) participate closely (Li and Friedman 1999). TGF$-\beta_1$ is mainly released from inflammatory cells, most likely Kupffer cells and neutrophils. It is widely accepted that TGF$-\beta_1$ activates and transforms hepatic stellate cells (HSC; Ito cells, lipocytes, vitamin A-storing cells) into myofibroblast-like cells. The transformed HSC secrete the amino acid, hydroxyproline, which is abundant in collagen-structured and extracellular matrix (ECM) fibrotic tissue. In turn, the HSC transformation induces the augmentation of ECM synthesis (Schafer et al. 1987; Nakatsukasa et al. 1990; Gressner 1996). Transformed HSC characteristically express alpha-smooth muscle

actin (α-SMA) (Enzan et al. 1994). Increased ECM synthesis leads to the progression of fibrosis. Therefore, the inhibition of hepatic damage potentially diminishes both inflammatory cell infiltration (*i.e.* Kupffer cells and neutrophils) and platelet aggregation. Consequently, the secretion of TGF−β_1 by those inflammatory cells should be reduced, the activation and transformation of myofibroblasts should be decreased and hepatic fibrosis/cirrhosis should diminish (Friedman 1993).

In a previous study, Dinçcer et al. (2002) observed that acute taurine treatment reduced the degree of CCl_4-mediated lipid peroxidation and liver necrosis. However, there is little information on the effect of taurine on chronic hepatic damage and oxidative stress mediated by repetitive administration of CCl_4. Furthermore, the effect of taurine on the activation of HSC remains unclear. Therefore, in the present study, we proposed to examine the effects of taurine on hepatic fibrosis and oxidative damage in a hepatic damage rat model induced by chronic CCl_4 administration and on fibrogenesis and oxidative stress in isolated rat HSC.

30.2 Materials and Methods

30.2.1 Animal Model Experiment

30.2.1.1 Hepatic Disease Rat Model

Male 6-week old rats (Sprague-Dawley; Japan SLC, Shizuoka, Japan) were divided randomly into 3 groups: normal ($N = 8$), liver disease (LD: $N = 18$), and LD treated with taurine (LDT: $N = 18$). The rats in the LDT group were given 2% taurine mixed with standard diet. After 1 week, the rats in the LD and LDT groups were subcutaneously injected 50% CCl_4-olive oil solution as 1 mL/kg body weight twice a week for 5 weeks. As in other studies, they also received 0.05% phenobarbital dissolved in the drinking water (Matsuzaki et al. 2002b; Miyazaki et al. 2003a, b; Miyazaki et al.2004b; Miyazaki et al. 2005; Zhang et al. 2006). Blood and liver were collected from the anesthetized animals. Taurine content was measured by amino acid analysis (Matsuzaki et al. 2002a, 2002b). All rats were kept at 21–25°C under 12-hour dark/light cycles, and received humane care in accordance with *The Guidelines of the University of Tsukuba for the Care of Laboratory Animals.*

30.2.1.2 Fibrosis Analysis

For histological analysis, the liver tissue was embedded on paraffin for Hematoxin & Eosin (HE) and silver staining, and immunohistrochemical (IHC) staining for $\alpha - SMA$. Hepatic fibrosis was quantified from positive silver staining as described in a previous study (Ludwig 1993).

Hepatic hydroxyproline content was used as a measure of fibrosis. Homogenized liver was incubated with 6N HCl at 105°C for 18 hours and centrifuged to get bottom's layer. After drying the pellet, the sample was incubated with chloramine-T

solution at 50°C for 90 min, and the hepatic hydroxyproline concentration was determined by measuring the absorbance at 540 nm by a 96-well plate reader.

TGF–β_1 mRNA content in the liver samples was quantified by real-time PCR. After reverse-transcription of RNA, hepatic TGF–β_1 mRNA content was detected using TaqMan® Universal PCR Master Mix (Perkin Elmer) and an Automated Sequence Detection System (Perkin Elmer). The temperature profile and the sequence of primers and probes for TGF–β_1 and β-actin (internal standard) are as follows: at 50°C for 2 min, at 95°C for 10 min, 40 cycles of at 95°C for 15 sec and at 60°C for 1 min, TGF–β_1 probe; 5'-AGT GGC TGA ACC AAG GAG ACG GAA TAC-3', TGF–β_1 sense primer; 5'-CGC CTG CAG AGA TTC AAG TCA A-3', TGF–β_1 anti-sense primer; 5'-GTC GGT TCA TGT CAT GGA TGG T-3', β-actin probe; 5'-TTT GAC ACC TTC AAC ACC CCA GCC A-3', β-actin sense primer; 5'-CGT GAA AAG ATG ACC CAG ATC A-3', β-actin anti-sense primer; 5'-ACA CAG CCT GGA TGG CTA CGT A-3'. The 5' and 3' terminals in both probes were FAM and TAMRA labeled, respectively. The β-actin probe was designed and provided by Nippon Flour Mills Co., Ltd. (Tokyo, Japan).

The expression of $\alpha - SMA$ protein was determined by Western blotting of homogenized liver.

30.2.1.3 Oxidative Stress Markers

The concentration of lipid hydroperoxide (LPO) and 8-hydroxy-2'-deoxyguanosine (8-OHdG) in serum and liver were used to assess lipid peroxidation and oxidative DNA damage, respectively. The LPO concentration was measured as hydroperoxides utilizing a redox reaction with ferrous ions (Mihaljevic et al. 1996) as described in the LPO assay kit (Cayman chemical company, Ann Arbor, MI). The 8-OHdG concentration was determined using the ELISA detection kit (8-OHdG Check; Japan Institute for the Control of Aging, Shizuoka, Japan).

30.2.2 Hepatic Satellite Cells Experiment

30.2.2.1 Isolation and Culture of HSC

HSC were isolated from normal Sprague-Dawley rat (Japan SLC) by the two-step collagenase perfusion method as described in our previous study (Zhang et al. 2006). Isolated HSC were plated on a 96-well plate at 1×10^4 cells/well and in 35mm plastic culture dishes at 5×10^5 cells/dish and incubated with DMEM containing 10% fetal bovine serum and 100 U/mL penicillin/streptomycin. HSC were cultured at 37°C in a humidified atmosphere of $5\% CO_2$. Activation of HSC was preliminary confirmed after $3 \sim 7$ days of plating, as determined by the loss of vitamin A autofluorescence and the increased expression of $\alpha - SMA$. After 24 hours in culture, the HSC were cultured for an additional 3 days (condition A) and 6 days (condition C) with 0, 25, and 50mM (Tau-0, -25, and -50) taurine, or for an additional 3 days with taurine followed by 3 days of culture without taurine (condition B). The culture

medium was changed every 2 days. The HSC were then harvested. In addition, culture medium before and after the completion of protocols B and C was kept for assays of LPO and hydroxyproline.

30.2.2.2 HSC Proliferation

Cell growth and DNA synthesis were measured by the MTT assay and the $5-bromo-2'$-deoxyuridine (BrdU) cell proliferation assay (Merck Biosciences, Darmstadt, Germany), respectively. Signaling protein expression associated with cell proliferation, such as the total and phosphorylated forms of MAPKs and Akt were determined by Western blotting. The antibodies used were raised against either total or the phosphorylated forms: Thr^{202}/Tyr^{204} p44/42 MAPK, Thr^{180}/Tyr^{182} p38 MARK, Thr^{183}/Tyr^{185} stress activated protein kinase/c-Jun N-terminal kinase (SAPK/JNK) and Ser^{473} Akt, respectively (Cell Signaling Technology, VA).

30.2.2.3 Transforming of HSC, Fibrogenesis, and Oxidative Stress Assays

In the harvested HSC subjected to condition A, the expression levels of $\alpha - SMA$ protein and TGF$-\beta_1$ mRNA was detected by Western blotting and real-time PCR, respectively, as described above. The LPO and hydroxyproline concentrations were determined in the culture medium collected before and after incubation with taurine.

30.2.3 Statistical Analysis

All data are presented as the means $\pm SD$. Significant differences were determined by the unpaired student's t-test, the one-way ANOVA post hoc Fisher's PLSD test or the Mann-Whitney U-test. Statistical significance was set at $p < 0.05$.

30.3 Results

30.3.1 CCl_4-Exposed Rats Treated with Taurine

30.3.1.1 Blood Biochemical Analysis and Taurine Concentration

Serum aspartate aminotransferase (AST) and alanine aminotransferase (ALT) were significantly increased in the LD group compared to that of the normal and LDT group, although ALT levels of the LDT were significantly higher than those of the normal group (Fig. 30.1). Total serum bilirubin content was increased eight-ten-fold in the LD and LDT groups compared to that of the normal, however there was no significant difference between the LD and LDT groups. Furthermore, serum albumin levels in the LD and LDT groups tended to be lower than those of the normal group; there was no significant difference between the LD and LDT groups. Serum taurine concentration of the LD group was unchanged relative to the normal, but levels

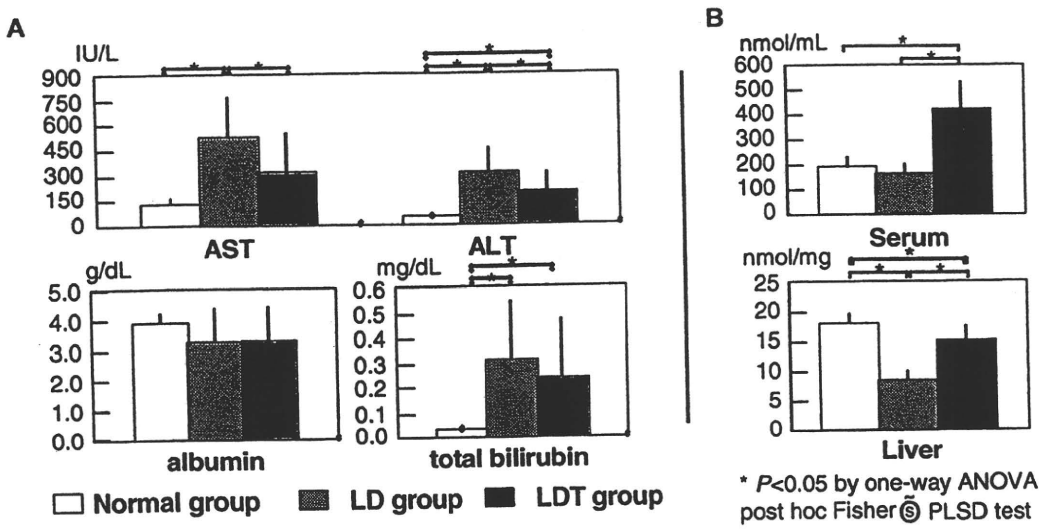

Fig. 30.1 Blood biochemical analyses and taurine concentration in serum and liver of CCl_4-treated rats with or without dietary taurine supplementation. **A**: Serum analysis of liver function, **B**: Taurine concentration in serum and liver. Data represent means ±SD

of the LDT groups were increased more than two-fold compared to those of the normal and LD groups (Fig. 30.1B). On the other hand, hepatic taurine content was significantly decreased in the LD group compared to that of the normal group; oral taurine administration preserved hepatic taurine levels against depletion observed in the LD group.

30.3.1.2 Histological Hepatic Pathology

Based on HE staining, CCl_4-administered rat livers underwent fibrosis, marked fatty degeneration, necrosis, cellular inflammation and infiltration of inflammatory cells including macrophages and lymphocytes. In the LD group, this damage was found throughout the liver and fibrotic infiltrations appeared in both the pericentral and periportal regions, with bridging fibrosis seen (Fig. 30.2). In the LDT group, hepatic necrosis and infiltration of inflammatory cells were inhibited compared to the LD group, particularly in the pericentral region. Similarly, the development of hepatic fibrosis was diminished in the pericentral region, the degree of bridging fibrosis was

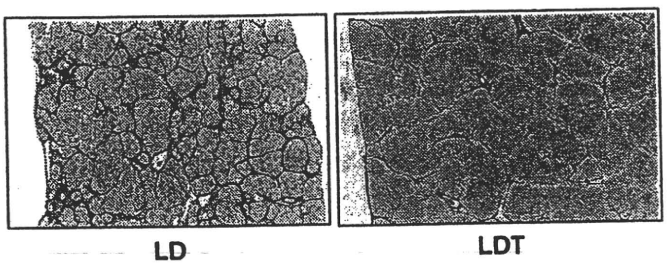

Fig. 30.2 Light micrographs of silver stained liver. Objective was ×5

Table 30.1 Parameters of fibrogenesis and oxidative stress in serum and liver tissue

Parameter	tissue	(unit)	Normal group	LD group	LDT group
Hydroxyproline	liver	(μg/L)	16.10 ± 6.04	304.83 ± 128.77[a]	212.27 ± 81.49[ab]
TGF−β_1 mRNA	liver		0.03 ± 0.01	0.98 ± 0.25[a]	0.45 ± 0.25[ab]
LPO	serum	(μmol/L)	1.11 ± 0.68	12.40 ± 5.09[a]	3.04 ± 1.91[ab]
	liver	(μmol/L)	0.88 ± 0.59	31.70 ± 11.35[a]	14.86 ± 14.2[ab]
8-OHdG	serum	(μmol/L)	1.58 ± 0.55	15.27 ± 4.7[a]	11.71 ± 4.41[ab]
	liver	(ng/g)	1.76 ± 0.39	9.27 ± 2.48[a]	6.88 ± 0.95[ab]

TGF−β_1 mRNA is expressed relative to β-actin mRNA. a and b show significant difference ($P < 0.05$) compared to the normal and LD groups, respectively, by one-way ANOVA post hoc Fisher's PLSD test. Data represent means±SD.

significantly reduced, and the architecture of the hepatic parenchyma and lobules was preserved. The fibrotic area quantified from the positive silver staining was 21.6 ± 9.1% in the LD group and 8.0 ± 5.9% in the LDT group, although there was no significant difference between the groups. Based on Western blot analysis and IHC staining, the number and intensity of α-SMA of the LD group was markedly increased compared to those of the LDT group.

30.3.1.3 Fibrogenesis and Oxidative Stress Markers

Hepatic hydroxyproline content and TGF−β_1 mRNA levels of the LD and LDT groups were significantly increased compared to those of the normal group, with the levels being significantly lower in the LDT group than in the LD group (Table 30.1). Likewise, the LPO and 8-OHdG content of serum and liver was significantly increased in both the LD and LDT groups compared to that of the normal group, but content was significantly lower in the LDT group than in the LD group.

30.3.2 Primary HSC Cultured with Taurine

30.3.2.1 HSC Proliferation and Signaling Pathways of Cell Growth

Cell growth of HSC assessed by the MTT assay was significantly decreased in cells cultured with 50 mM taurine compared to those cultured without taurine (Fig. 30.3). There was also a significant difference between cells incubated with medium containing 25 mM taurine for 6 days (condition C) compared to those cultured without taurine. Similarly, based on the BrdU assay, DNA synthesis of the 50 mM taurine group was significantly reduced compared to that of the 0 mM taurine group. For conditions B and C, DNA synthesis was significantly lower in the 50 mM taurine group than in the 25 mM taurine group. HSC incubated with taurine according to condition A showed no significant difference in total and phosphorylated forms of the MAPKs and Akt.

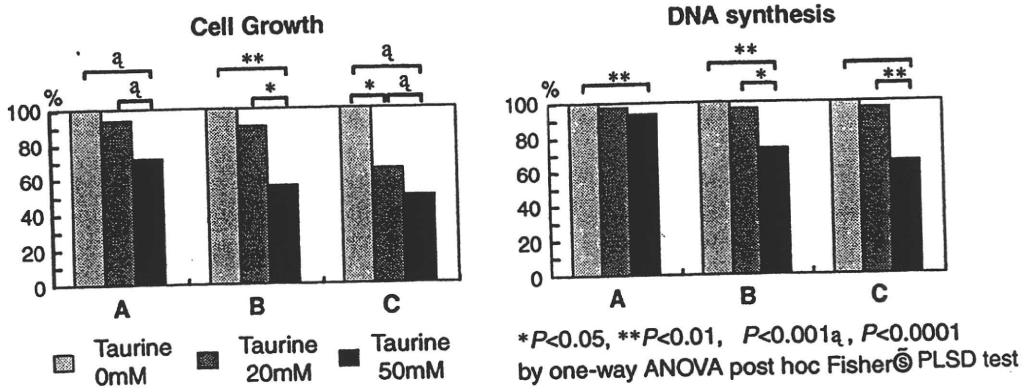

Fig. 30.3 Cell proliferation of primary cultured HSC treated with taurine. Cell growth and DNA synthesis were analyzed by MMT and BrdU assays. **Condition A:** cultured with taurine for 3 days, **Condition B:** cultured with taurine for 3 days followed by 3 days without taurine, **Condition C:** cultured with taurine for 6 days. Data represent means±SD

30.3.2.2 Fibrogenesis and Oxidative Stress Factors of Cultured HSC

When incubated according to condition A, TGF−β_1 mRNA content of TAU-25 (0.02 ± 0.01 fold compared to β-actin) and -50 (0.03 ± 0.01) was significantly decreased compared to that of Tau-0 (0.04 ± 0.03, $P < 0.05$). However, there was no significant difference between the Tau-25 and -50 groups. The LPO and hydroxyproline content of culture medium collected before (Pre) and after treatment with taurine for 3 days (condition A) was higher in the Tau-0 (0.48±0.07 g/L and 7.16±3.85 μ mol/L, respectively) than in the Pre group (0.04 ± 0.01, $P < 0.01$ and 1.92 ± 0.39, $P < 0.05$, respectively). The hydroxyproline concentration (g/L) was significantly lower in the Tau-50 (0.38 ± 0.08, $P < 0.05$) than in the Tau-0 group. The LPO concentration (μ mol/L) in the Tau-25 (4.84 ± 2.53, $P < 0.05$) and -50 (3.13 ± 2.50, $P < 0.01$) groups was significantly decreased compared to those of the Tau-0 group. There was no significant difference between the hydroxyproline and LPO concentrations of the Tau-25 and -50 groups.

30.4 Discussion

In the present study, taurine treatment prevented the decline in hepatic taurine content of the CCl_4 treated rat. Taurine treatment also protected the liver against oxidative stress-induced damage trigger by repetitive CCl_4 administration in rats. Particularly noteworthy was the reduction in hepatic fibrosis of the CCl_4-administered rats treated with taurine. Furthermore, in the cultured HSC study, taurine inhibited the transformation of HSC while reducing oxidative stress. These results showed that fibrosis was directly inhibited by taurine through attenuation of oxidative stress-mediated transformation of HSC to myofibroblast-like cells. However, the mechanism of taurine-mediated modulation of cell proliferation of HSC remains unclear, but does not appear to involve the signaling pathways of MAPKs and

Akt. Therefore, there must be some other mechanism that can mediate the effect of taurine on HSC proliferation. Furthermore, the mechanism underlying taurine-mediated protection against liver disease must involve multiple factors because taurine diminished diverse types of hepatic damage, including hepatocyte necrosis, fatty degeneration, infiltration of inflammatory cells and fibrosis. Therefore, taurine acts through multiple and complex mechanisms, including cell membrane stabilization, osmoregulation, detoxification, anti-apoptosis, modulation of bile acid conjugation/excretion, cholesterol excretion, anti-inflammation, anti-oxidation, inhibition of fibrogenesis and cytokine secretion, inhibition of HSC transformation and inhibition of cytokine/autocrine action. In conclusion, taurine supplementation should be considered as a therapy to lessen the severity of oxidative stress-induced hepatic injury and fibrosis.

Acknowledgments This study was supported by a research grant from Taisho Pharmaceutical Co., Ltd. Japan. This study has been previously published in part in the *Journal of Hepatology* in 2005.

References

Awapara J (1956) The taurine concentration of organs from fed and fasted rats. J Biol Chem 218(2):571-6.

Azuma J, Hamaguchi T, Ohta H, Takihara K, Awata N, Sawamura A, Harada H, Tanaka Y, Kishimoto S (1987) Calcium overload-induced myocardial damage caused by isoproterenol and by adriamycin: possible role of taurine in its prevention. Adv Exp Med Biol 217:167–179

Balkan J, Dogru-Abbasoglu S, Kanbagli O, Cevikbas U, Aykac-Toker G, Uysal M (2001) Taurine has a protective effect against thioacetamide-induced liver cirrhosis by decreasing oxidative stress. Hum Exp Toxicol 20:251–254

Danielsson H (1963) Present status of research on catabolism, excretion of cholesterol. Adv Lipid Res 1:335–385

Davison AN, Kaczmarec LK (1971) Taurine-a possible neurotransmitter? Nature 234:107–108

Dinçcer S, Özenirler S, Öz E, Akyol G, Özogul C (2002) The protective effect of taurine pretreatment on carbon tetrachloride-induced hepatic damage – A light and electron microscopic study. Amino Acids 22:417–426

Enzan H, Himeno H, Iwamura S, Saibara T, Onishi S, Yamamoto Y, Hara H (1994) Immunohistochemical identification of Ito cells and their myofibroblastic transformation in adult human liver. Virchows Arch 424:249–256

Friedman SL (1993)Seminars in medicine of the Beth Israel Hospital, Boston. The cellular basis of hepatic fibrosis. Mechanisms and treatment strategies. N Engl J Med 328:1828–1835

Fukuda K, Hirai Y, Yoshida H, Nakajima T, Usui T (1982) Free amino acid content of lymphocytes and granulocytes compared. Clin Chem 28:1758–1761

Gordon RE, Heller RF, Heller RF (1992) Taurine protection of lungs in hamster models of oxidant injury: a morphologic time study of paraquat and bleomycin treatment. Adv Exp Med Biol 315:319–328

Green TR, Fellman JH, Eicher AL, Pratt KL (1991) Antioxidant role and subcellular location of hypotaurine and taurine in human neutrophils. Biochim Biophys Acta 1073:91–97

Gressner AM (1996) Transdifferentiation of hepatic stellate cells (Ito cells) to myofibroblasts: a key event in hepatic fibrogenesis. Kidney Int Suppl 54:S39–S45

Hosokawa Y, Matsumoto A, Oka J, Itakura H, Yamaguchi K (1990) Isolation and characterization of a cDNA for rat liver cysteine dioxygenase. Biochem Biophys Res Commun 168:473–478

Huxtable RJ (1980) Does taurine have a function? Fed Proc 39:2678–2679
Huxtable RJ (1992) Physiological actions of taurine. Physiol Rev 72:101–163
Jacobsen JG, Swimth LH (1968) Biochemistry and physiology of taurine and taurine derivatives. Physiol Rev 48:424–511
Kaisaki PJ, Jerkins AA, Goodspeed DC, Steele RD (1995) Cloning and characterization of rat cysteine sulfinic acid decarboxylase. Biochim Biophys Acta 1262:79–82
Kanner BI, Nurit KD (1994) Structure and function of sodium-coupled neurotransmitter transporters. Cell Physiol Biochem 4:174
Koyama I, Nakamura T, Ogasawara M, Nemoto M, Yoshida T (1992) The protective effect of taurine on the biomembrane against damage produced by the oxygen radical. Adv Exp Med Biol 315:355–359
Kuriyama K (1980) Taurine as a neuromodulator. Fed Proc 39:2680–2684
Li D, Friedman SL (1999) Liver fibrogenesis and the role of hepatic stellate cells: new insights and prospects for therapy. J Gastroenterol Hepatol 14:618–633
Ludwig J (1993) The nomenclature of chronic active hepatitis:an obituary. Gastroenterol 105: 274–278
Matsuzaki Y, Miyazaki T, Miyakawa S, Bouscarel B, Ikegami T, Tanaka N (2002a) Decreased taurine concentration in skeletal muscles after exercise for various durations. Med Sci Sports Exerc 34:793–797
Matsuzaki Y, Miyazaki T, Ohkoshi N, Miyakawa S, Bouscarel B, Tanaka N (2002b) Degeneration of skeletal muscle fibers in the rat administrated carbon tetrachloride:similar histological findings of the muscle in a 64-year-old patient of LC with muscle cramp. Hepatol Res 24:368–378
Mihaljevic B, Katusin-Razem B, Razem D (1996) The reevaluation of the ferric thiocyanate assay for lipid hydroperoxides with special considerations of the mechanistic aspects of the response. Free Radic Biol Med 21:53–63
Miyazaki T, Ikegami T, Zhang Y, Honda A, Doy M, Matsuzaki Y (2005) The prevention mechanisms of taurine on hepatic damage and fibrosis via antioxidative stress. Jpn Pharmacol Ther 33:S105
Miyazaki T, Matsuzaki Y, Ikegami T, Miyakawa S, Doy M, Tanaka N, Bouscarel B (2004a) Optimal and effective oral dose of taurine to prolong exercise performance in rat. Amino Acids 27:291–298
Miyazaki T, Matsuzaki Y, Ikegami T, Miyakawa S, Doy M, Tanaka N, Bouscarel B (2004b) The harmful effect of exercise on reducing taurine concentration in the tissues of rats treated with CCl_4 administration. J Gastroenterol 39:557–562
Miyazaki T, Matsuzaki Y, Karube M, Bouscarel B, Miyakawa S, Tanaka N (2003a) Amino acid ratios in plasma and tissues in a rat model of liver cirrhosis before and after exercise. Hepatol Res 27:230–237
Miyazaki T, Matsuzaki Y, Karube M, Miyakawa S, Tanaka N (2003b) Clinical importance of taurine maintenance on liver disease. Gastroenterology 37:558–562
Nakashima T, Seto Y, Nakajima T, Shima T, Sakamoto Y, Cho N, Sano A, Iwai M, Kagawa K, Okanoue T, et al. (1990) Calcium-associated cytoprotective effect of taurine on the calcium and oxygen paradoxes in isolated rat hepatocytes. Liver 10:167–172
Nakatsukasa H, Nagy P, Evarts RP, Hsia CC, Marsden E, Thorgeirsson SS (1990) Cellular distribution of transforming growth factor-beta 1 and procollagen types I, III, and IV transcripts in carbon tetrachloride- induced rat liver fibrosis. J Clin Invest 85:1833–1843
Nieminen ML, Tuomisto L, Solatunturi E, Eriksson L, Paasonen MK (1988) Taurine in the osmoregulation of the Brattleboro rat. Life Sci 42:2137–2143
Pasantes MH, Wright CE, Gaull GE (1984) Protective effect of taurine, zinc and tocopherol on retinol-induced damage in human lymphoblastoid cells. J Nutr 114:2256–2261
Pasantes MH, Wright CE, Gaull GE (1985) Taurine protection of lymphoblastoid cells from iron-ascorbate induced damage. Biochem Pharmacol 34:2205–2207
Reymond I, Sergeant A, Tappaz M (1996) Molecular cloning and sequence analysis of the cDNA encoding rat liver cysteine sulfinate decarboxylase (CSD). Biochim Biophys Acta 1307: 152–156

Schafer S, Zerbe O, Gressner AM (1987) The synthesis of proteoglycans in fat-storing cells of rat liver. Hepatology 7:680–687

Sjovall J (1959) Dietary glycine and taurine on bile acid conjugation in man; bile acids and steroids 75. Proc Soc Exp Biol Med 100:676–678

Sturman JA (1993) Taurine in development. Physiol Rev 73:119–147

Tappaz M, Bitoun M, Reymond I, Sergeant A (1999) Characterization of the cDNA coding for rat brain cysteine sulfinate decarboxylase: brain and liver enzymes are identical proteins encoded by two distinct mRNAs. J Neurochem 73:903–912

Timbrell JA, Seabra V, Waterfield CJ (1995) The in vivo and in vitro protective properties of taurine. Gen Pharmacol 26:453–462

Vohra BP, Hui X (2001) Taurine protects against carbon tetrachloride toxicity in the cultured neurons and in vivo. Arch Physiol Biochem 109:90–94

Wang QJ, Giri SN, Hyde DM, Li C (1991) Amelioration of bleomycin-induced pulmonary fibrosis in hamsters by combined treatment with taurine and niacin. Biochem Pharmacol 42:1115–1122

Waterfield C.J, Mesquita M, Parnham P, Timbrell J.A (1993a) Taurine protects against the cytotoxicity of hydrazine, 1,4-naphthoquinone and carbon tetrachloride in isolated rat hepatocytes. Biochem Pharmacol 46:589–595

Waterfield CJ, Turton JA, Scales MD, Timbrell JA (1993b) Reduction of liver taurine in rats by beta-alanine treatment increases carbon tetrachloride toxicity. Toxicology 29:7–20

Wright CE, Lin TT, Lin YY, Sturman JA, Gaull GE (1985) Taurine scavenges oxidized chlorine in biological systems. Prog Clin Biol Res 179:137–147

Zhang Y, Ikegami T, Honda A, Miyazaki T, Bouscarel B, Rojkind M, Hyodo I, Matsuzaki Y (2006) Involvement of integrin-linked kinase in carbon tetrachloride-induced hepatic fibrosis in rats. Hepatology 44:612–622

70 (140)　　2009 Vol. 54 No. 2

自己免疫性肝疾患類似GVHRマウスモデルの肝病変に対する制御性T細胞の関与

東京医科大学地域医療振興学寄付講座[1)],
東京医科大学茨城医療センター共同研究センター[2)],
茨城県立中央病院[3)], 東京医科大学茨城医療センター消化器内科[4)],
霞ヶ浦成人病研究事業団[5)]
宮﨑　照雄[1,2)], 土井　幹雄[3)], 伊藤　進一[4,5)], 本多　彰[1,2)]
池上　正[4)], 松﨑　靖司[1,4)]

はじめに

われわれはこれまで，肝特異的マウス移植片対宿主反応(GVHR)モデルを作製し，自己免疫性肝疾患の病態解析を行ってきた[1-4)]。GVHRモデルは，C57BL/6(B6)雄マウスとMHC class IIの3つのアミノ酸の異なるB6.C-H-$2^{bm/2}$雌マウスを交配して得られたF1雌マウスに，B6雌マウスの脾臓より分離した1×10^7個のT細胞を尾静脈へ注射することで作製される(図1)。その結果，胆管上皮細胞に異所性にMHC class IIの発現がみられ，自己免疫機序が関与した門脈域，中心静脈周囲にrecipients由来のリンパ球を中心とした炎症性細胞浸潤が認められる。また，自己抗体(抗核抗体，抗ミトコンドリア抗体)の産生が確認される。肝組織への炎症性細胞浸潤は，GVHR導入後5目より確認され，その後，2週目でピークを迎える。しかし，GVHR導入2週目以降，自然経過観察下で炎症性細胞浸潤面積，浸潤部位数共に有意に減少し，線維化や肝硬変には至らず改善してしまう。このモデル特有のGVHR導入後一過性の炎症からの改善のメカニズムを明らかにすることは，自己免疫性肝疾患の病態解明への一助になると考えられる。

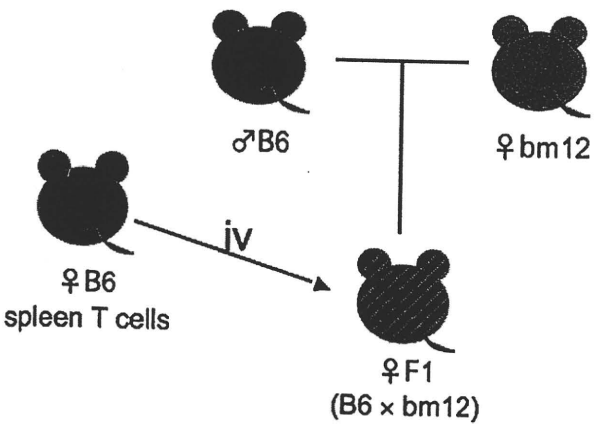

図1　マウスGVHRモデル

今研究では，このGVHRモデル肝病変改善の原因を明らかにする目的で，肝組織内の免疫寛容獲得過程に関与する遺伝子群について，網羅的遺伝子発現頻度解析とその結果に基づいて浸潤内炎症性細胞群に対して免疫組織的解析を行った。

方　法

GVHR導入直後，2，4，8週目(G0，G2，G4，G8)のマウスより肝組織を採取した。遺伝子解析には，G0，G2，G8を用い，同週令の正常マウスをコントロールとし，炎症性サイトカイン関連遺伝子514種についてシグマ社のPanorama® Mouse Cytokine Gene Arrayを用いた。whole liverからtotal RNAを抽出し，逆転写の際にcDNAに[α-^{33}P]dCTPをラベル化させ，そのcDNAをgene arrayにhybridizationさせた。spotの強度は，normalization後，2倍以上の強度を増加，1/2倍以上を減少とした。

組織学的解析は，G0，G2，G4，G8から採取した肝組織からパラフィン切片を作製し，HE染

色と浸潤リンパ球に対しCD4，CD8，CD20，CD25，CD45ro，CD161，IL-10レセプター[R]β，FoxP3の免疫染色を行い，各陽性細胞数の定量を行った。また，制御性T(Treg)細胞表面マーカー(CD4，CD25，CD161，IL-10Rβ)において，蛍光二重免疫染色を行った。

更に，免疫組織学解析の結果を検証するため，F1マウスに抗IL-10抗体もしくはモノクローナル抗体(Rat IgG Isotype)を腹腔内に投与し，その4時間後，GVHR導入を行い，その後2週目の肝病態変化を観察した(**図2**)。

結　果

Gene arrayの解析の結果，514遺伝子の変化は3パターンに分類された。G0からG8まで変化がないパターンに，448遺伝子が該当した。それ以外は，G0に比しG2で増加し，その後，G8で減少するパターンの20遺伝子と，G8まで維持するパターンの46遺伝子であった。ちなみに，G0からG2で減少，G2からG8で増加するパターンはなかった。病態改善と共に変動するパターンの20遺伝子のうち，G2時点で最も発現が高い遺伝子は，IL-2Rγであった。この結果から，IL-2Rの一部を共に構成するIL-2Rα(CD25)との関わりあいを推測し，近年，自己免疫疾患などの免疫寛容破綻への免疫制御が注目されているTreg細胞($CD4^+CD25^+$T細胞，$CD161^+$NKT細胞，$IL\text{-}10R^+$Tr1細胞など)に着目するに至った。

免疫染色の結果，肝組織内浸潤炎症性細胞群にTreg細胞マーカー(CD25，FoxP3，IL-10R，CD161)を含め，今研究で検討した表面マーカーすべてにおいて，陽性細胞が認められた(**図3**)。

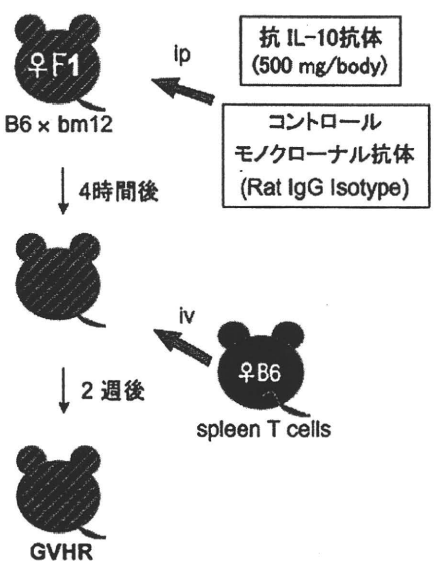

図2　抗IL-10抗体投与GVHRマウス

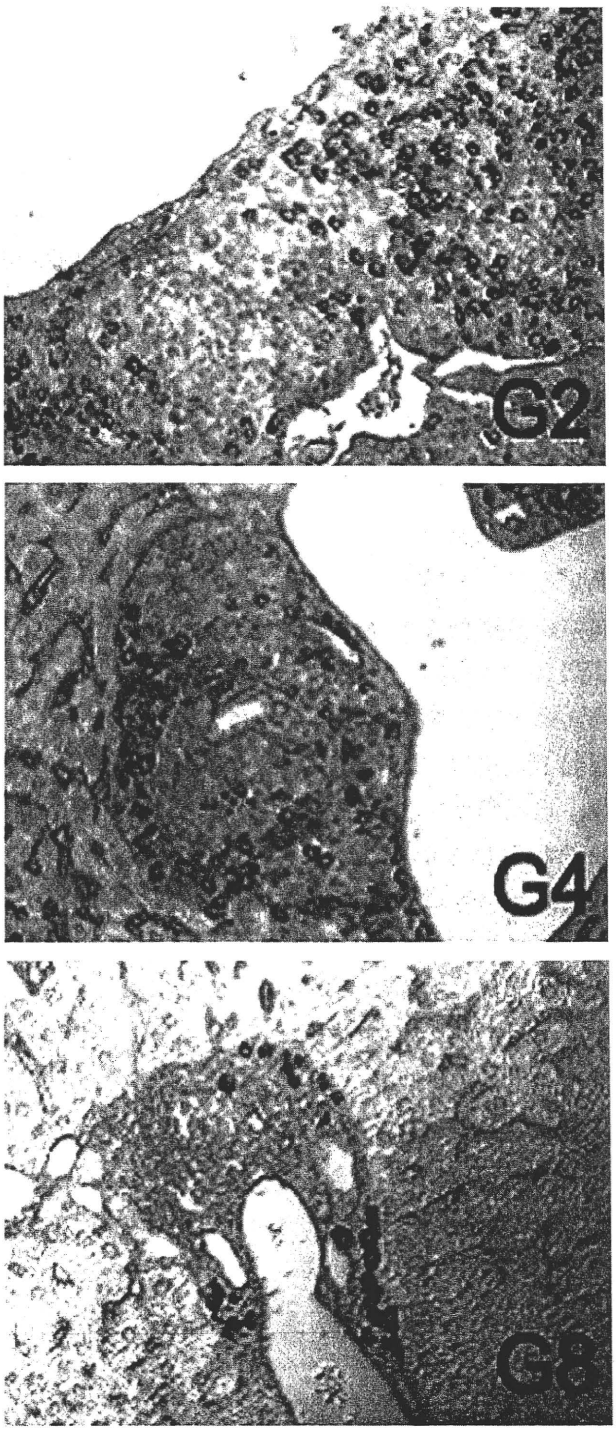

図3　肝組織内浸潤CD4陽性細胞免疫染色像

更に，蛍光二重染色の結果，Treg 細胞マーカーは，それぞれ CD4 との共発現がみられ，免疫染色による陽性細胞が Treg 細胞であることを確認した。

G2，G4，G8 における各マーカー陽性細胞数は，肝病態改善と共に G2 から G8 にかけ有意に減少した。しかし，IL-10R$^+$ 細胞のみ，G8 までの発現量が維持していた。

そこで，GVHR の病態改善に対する Tr1 細胞発現の意義を抗 IL-10 抗体投与 GVHR マウスにおいて確認した。抗 IL-10 抗体投与により，GVHR マウスの肝組織内炎症性細胞浸潤域に IL-10R$^+$ 細胞浸潤は完全に抑制された。それに伴い，モノクローナル抗体投与 GVHR マウスと比較して，炎症性細胞浸潤が有意に増悪した。また，抗 IL-10 抗体投与 GVHR マウス肝組織内において，FoxP3$^+$ 細胞の有意な浸潤増加が観察された。

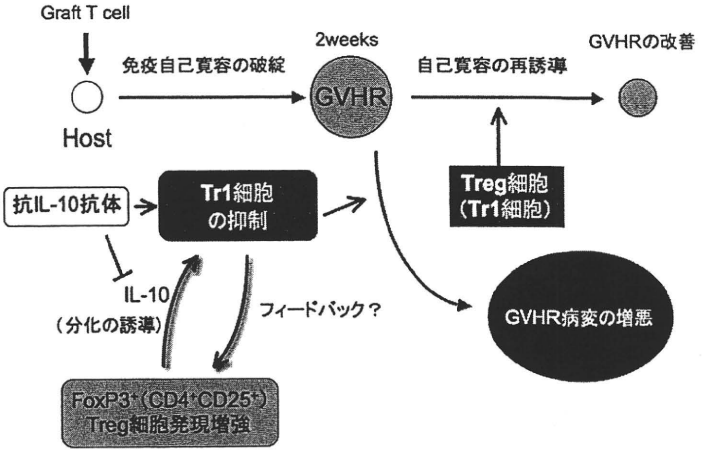

図 4　GVHR モデルにおける Treg 細胞の免疫寛容制御機序

考察・結論

遺伝子解析ならびに免疫組織化学染色の結果，GVHR モデル肝組織内に Treg 細胞の出現が認められ，病態改善過程において Tr1 細胞の発現が持続していた。このことから，GVHR 導入後，自己免疫寛容の破綻が生じ，肝に炎症性細胞浸潤が生じるが，この Tr1 細胞が関与することで自己免疫寛容が再獲得され，病態が一過性のものとして生じている可能性が示唆された(**図 4**)。これは，抗 IL-10 抗体投与 GVHR マウスで，Tr1 細胞の肝内浸潤領域内での発現を抑制させたところ，炎症性細胞浸潤が増悪したことから，病態改善への Tr1 細胞の関与を大きく支持するものと考えられる。また，IL-10 抗体投与 GVHR マウスで，FoxP3$^+$ 細胞の浸潤が有意に増加したのは，発現抑制された Tr1 細胞の末梢組織での分化を促進するためのフィードバックによるものと推測される[5,6]。

文　献

1) Itoh S, Matsuzaki Y, Kimura T, *et al.*: Cytokine profile of liver-infiltrating CD4$^+$ T cells separated from murine primary biliary cirrhosis-like hepatic lesions induced by graft-versus-host reaction. J Gastroenterol Hepatol 2000; **15**: 443-451.
2) Itoh S, Matsuzaki Y, Kimura T, *et al.*: Suppression of hepatic lesions in a murine graft-versus-host reaction by antibodies against adhesion molecules. J Hepatol 2000; **32**: 587-595.
3) Unno R, Matsuzaki Y, Itoh S, *et al.*: Novel murine autoimmune-mediated liver disease model induced by graft-versus-host reaction and concanavalin A. J Gastroenterol Hepatol 2001; **16**: 1149-1157.
4) Unno R, Matsuzaki Y, Itoh S, *et al.*: Progression of autoimmune-mediated hepatic lesions in a murine graft-versus-host reaction by neutralizing IL-10. Hepatol Res 2003; **26**: 354-361.
5) Thompson C, Powrie F: Regulatory T cells. Curr Opin Pharmacol 2004; **4**: 408-414.
6) Veldman C, Nagel A, Hertl M: Type I regulatory T cells in autoimmunity and inflammatory diseases. Int Arch Allergy Immunol 2006; **140**: 174-183.

methods

Highly sensitive quantification of serum malonate, a possible marker for de novo lipogenesis, by LC-ESI-MS/MS

Akira Honda,*,† Kouwa Yamashita,§ Tadashi Ikegami, Takashi Hara,†† Teruo Miyazaki,*,† Takeshi Hirayama,** Mitsuteru Numazawa,§ and Yasushi Matsuzaki[1,†,**]**

Center for Collaborative Research,* Department of Development for Community Medicine,† and Department of Gastroenterology,** Tokyo Medical University Ibaraki Medical Center, Ami, Ibaraki 300-0395, Japan; Faculty of Pharmaceutical Science,§ Tohoku Pharmaceutical University, Sendai, Miyagi 981-8558, Japan; and Ibaraki Prefectural Institute of Public Health,†† Mito, Ibaraki 310-0852, Japan

Abstract We describe a new sensitive and specific method for the quantification of serum malonate (malonic acid, MA), which could be a new biomarker for de novo lipogenesis (fatty acid synthesis). This method is based upon a stable isotope-dilution technique using LC-MS/MS. MA from 50 μl of serum was derivatized into di-(1-methyl-3-piperidinyl)malonate (DMP-MA) and quantified by LC-MS/MS using the positive electrospray ionization mode. The detection limit of the DMP-MA was approximately 4.8 fmol (500 fg) (signal-to-noise ratio = 10), which was more than 100 times more sensitive compared with that of MA by LC-MS/MS using the negative electrospray ionization mode. The relative standard deviations between sample preparations and measurements made using the present method were 4.4% and 3.2%, respectively, by one-way ANOVA. Recovery experiments were performed using 50 μl aliquots of normal human serum spiked with 9.6 pmol (1 ng) to 28.8 pmol (3 ng) of MA and were validated by orthogonal regression analysis. The results showed that the estimated amount within a 95% confidence limit was 14.1 ± 1.1 pmol, which was in complete agreement with the observed $\bar{X}_0$ = 15.0 ± 0.6 pmol, with a mean recovery of 96.0%. This method provides reliable and reproducible results for the quantification of MA in human serum.—Honda, A., K. Yamashita, T. Ikegami, T. Hara, T. Miyazaki, T. Hirayama, M. Numazawa, and Y. Matsuzaki. **Highly sensitive quantification of serum malonate, a possible marker for de novo lipogenesis, by LC-ESI-MS/MS.** ***J. Lipid Res.*** **2009.** 50: **2124–2130.**

Supplementary key words acetyl-CoA carboxylase • carnitine palmitoyl transferase 1 • fatty acid synthase • liquid chromatography-electrospray ionization-tandem mass spectrometry • malonic acid • malonyl-CoA • malonyl-CoA decarboxylase

Acetyl-CoA carboxylase (ACC) is the rate-controlling enzyme in the fatty acid biosynthetic pathway, and catalyzes the formation of malonyl-CoA from acetyl-CoA plus bicarbonate. Malonyl-CoA is not only substrate for fatty acid synthase (FAS) but is also a potent inhibitor of carnitine palmitoyl transferase 1 (1), the rate-limiting enzyme of fatty acid β-oxidation. Therefore, malonyl-CoA is a key molecule that controls fatty acid metabolism in the body. In addition, recent studies have shown that the level of hypothalamic malonyl-CoA is dynamically regulated by fasting and feeding and that it alters subsequent feeding behavior (2).

To determine ACC activity in tissues, an invasive tissue biopsy is necessary. However, whole body synthesis of fatty acid may be evaluated by the quantification of serum malonyl-CoA metabolites. This concept originates from our previous studies, which showed that serum concentrations of the immediate products of the rate-controlling enzymes in cholesterol and bile acid biosynthetic pathways reflected the activities of the rate-controlling enzymes and whole body cholesterol and bile acid biosynthesis (3). Furthermore, patients with malonyl-CoA decarboxylase (MCD) deficiency, who must have increased tissue malonyl-CoA concentrations, are characterized by markedly elevated urinary malonic acid (MA), called "malonic aciduria" (4). This phenomenon suggests that malonyl-CoA is easily hydrolyzed into MA by an unidentified tissue thioesterase(s). Therefore, we thought that serum MA concentrations might well reflect total body FAS.

This work was supported in part by a Grant-in-Aid for Scientific Research (C20591309) from the Japan Society for the Promotion of Science and a grant from the Ministry of Education, Culture, Sports, Science and Technology of Japan.

Manuscript received 1 December 2008 and in revised form 15 April 2009.

Published, JLR Papers in Press, April 29, 2009
DOI 10.1194/jlr.D800054-JLR200

Abbreviations: ACC, acetyl-CoA carboxylase; DMP-MA, Di-(1-methyl-3-piperidinyl)malonate; FAS, fatty acid synthase; MA, malonic acid (malonate); MCD, malonyl-CoA decarboxylase; MMA, methylmalonic acid (methylmalonate); N-ESI, ESI in negative mode; P-ESI, ESI in positive mode; SA, succinic acid (succinate); SRM, selected reaction monitoring.

[1]To whom correspondence should be addressed.
e-mail: ymatsuzaki-gi@umin.ac.jp

Although methodological reports for the quantification of serum MA are not available, there have been some reports that describe the methods for the determination of urinary MA levels in patients with MCD deficiency by gas chromatography (5, 6) or gas chromatography-mass spectrometry (7). In these methods, urinary organic acids were extracted with ethyl acetate and converted into trimethylsilyl derivatives before analysis. Alternatively, blood malonylcarnitine has been measured for the diagnosis of MCD deficiency using liquid chromatography-tandem mass spectrometry coupled with electrospray ionization mode (LC-ESI-MS/MS) (8). However, because all of these methods were developed to diagnose markedly elevated MA levels in patients with MCD deficiency, the authors did not pay significant attention to the sensitivities of the methods.

The aim of this study was to measure serum MA concentrations in normal human subjects with sufficient sensitivity and specificity. For this purpose, serum MA was derivatized into di-(1-methyl-3-piperidinyl)malonate (DMP-MA) and quantified using positive LC-ESI-MS/MS (LC-P-ESI-MS/MS).

MATERIALS AND METHODS

Chemicals

MA and [$^{13}C_3$]MA were purchased from Sigma-Aldrich Chemical Co. (St. Louis, MO). 3-Hydroxy-1-methylpiperidine and 2-methyl-6-nitrobenzoic anhydride were purchased from Tokyo Kasei Kogyo (Tokyo, Japan) and 4-dimethylaminopyridine and formic acid were obtained from Wako Pure Chemical Industries (Osaka, Japan). Additional reagents and solvents were of analytical grade.

Sample collection

Blood samples were collected from healthy human volunteers. After coagulation and centrifugation at 1,500 *g* for 10 min, serum samples were stored at −20°C until analysis. Informed consent was obtained from all subjects, and the experimental procedures were conducted in accordance with the ethical standards of the Helsinki Declaration. Rat serum was prepared in our previous study (9) and had been stored at −20°C until it was used in the present experiments.

Sample preparation

Fifty μl of serum was placed in a microcentrifuge tube (1.5 ml, Eppendorf, Hamburg, Germany), and 19.2 pmol (2 ng) of [$^{13}C_3$] MA in 100 μl of acetonitrile as an internal standard. The sample tube was vortexed for 1 min and centrifuged at 2,000 *g* for 1 min. The solution of internal standard in acetonitrile led to deproteinization of the sample and the liquid phase was collected and evaporated to dryness at 80°C under a nitrogen stream. Derivatization of MA into DMP-MA was performed according to the Shiina method for the synthesis of carboxylic esters (10) with some modifications. The reagent mixture for derivatization consisted of 2-methyl-6-nitrobenzoic anhydride (67 mg), 4-dimethylaminopyridine (20 mg), pyridine (900 μl), and 3-hydroxy-1-methylpiperidine (100 μl). The freshly prepared reagent mixture (100 μl) was added to the serum extract and the reaction mixture was allowed to stand at room temperature for 30 min. After the addition of 2 ml of n-hexane, the mixture was vortexed for 30 s and centrifuged at 700 *g* for 2 min. The clear supernatant was collected and evaporated at 80°C under nitrogen. The residue was redissolved in 50 μl of 1% formic acid in water and an aliquot (1 μl) was injected into the following LC-MS/MS system.

Determination of DMP-MA by LC-P-ESI-MS/MS

The LC-MS/MS system consisted of a TSQ Quantum Ultra quadrupole mass spectrometer (Thermo Fisher Scientific, San Jose, CA) equipped with an H-ESI probe and a Nanospace SI-2 HPLC system (Shiseido, Tokyo, Japan). Chromatographic separation was performed using a Hypersil GOLD aQ column (150 × 2.1 mm, 3 μm, Thermo Fisher Scientific) at 40°C. Initially, the mobile phase was comprised of 0.2% formic acid in water and was used at a flow rate of 200 μl/min for 5 min, and it was then switched to 0.2% formic acid in acetonitrile at a flow rate of 300 μl/min for an additional 3.5 min. The general LC-MS/MS conditions were as follows: spray voltage, 1000 V; vaporizer temperature, 350°C; sheath gas (nitrogen) pressure, 50 psi; auxiliary gas (nitrogen) flow, 40 arbitrary units; ion transfer capillary temperature, 350°C; collision gas (argon) pressure, 1.5 mTorr; collision energy, 15 V; and ion polarity, positive.

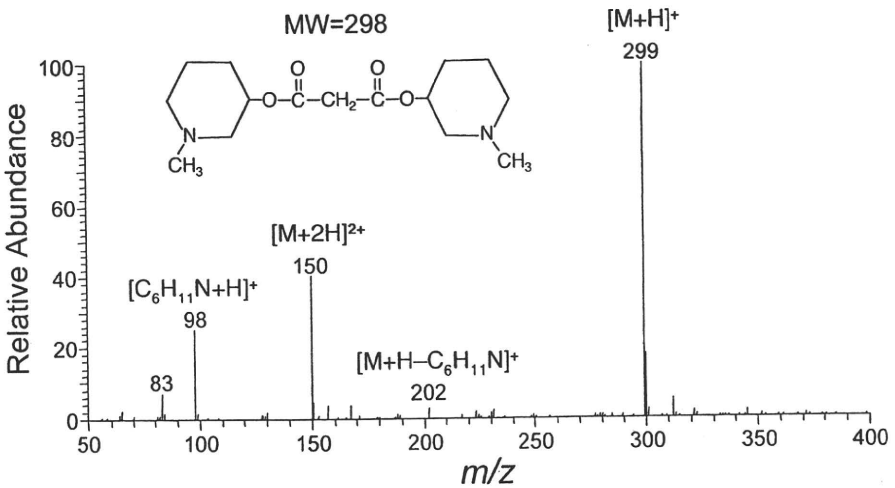

Fig. 1. Typical P-ESI mass spectrum of the DMP-MA. The general LC-MS/MS conditions were as described in Materials and Methods.

Determination of MA by LC-N-ESI-MS/MS

LC-negative (N)-ESI-MS/MS analysis of MA was carried out using the same LC-MS/MS instrument described above. Hypersil GOLD column (150 × 2.1 mm, 3 μm, Thermo Fisher Scientific) was used at 40°C. The mobile phase consisted of methanol-water (5:95, v/v) containing 0.2% formic acid and was used at a flow rate of 200 μl/min. The general LC-MS/MS conditions were as follows: spray voltage, 4000 V; vaporizer temperature, 350°C; sheath gas (nitrogen) pressure, 50 psi; auxiliary gas (nitrogen) flow, 30 arbitrary units; ion transfer capillary temperature, 300°C; collision gas (argon) pressure, 1.5 mTorr; collision energy, 15 V; and ion polarity, negative.

Statistics

Data are reported as the mean ± SD. Linearity of the calibration curve was analyzed by simple linear regression. Reproducibility was analyzed by one-way ANOVA (JMP software, SAS Institute, Inc., Cary, NC). The estimated amount ± 95% confidence limit was obtained as an index of precision (11). To calculate the values, orthogonal regression analysis was performed in the recovery study by using JMP software. For all analyses, significance was accepted at the level of $P < 0.05$.

RESULTS

Selected reaction monitoring

A typical ESI positive mass spectrum of the DMP-MA is shown in **Fig. 1**. This DMP ester derivative exhibited $[M+H]^+$ ion at *m/z* 299 as the base peak. In the MS/MS spectrum using *m/z* 299 as a precursor ion, the $[C_6H_{11}N+H]^+$ ion was observed at *m/z* 98 as the most prominent peak. The selected reaction monitoring (SRM) was conducted using *m/z* 299 → *m/z* 98 for the DMP-MA and *m/z* 302 → *m/z* 98 for the [$^{13}C_3$] variant. We also monitored *m/z* 299 → *m/z* 202, a product ion containing the MA molecule

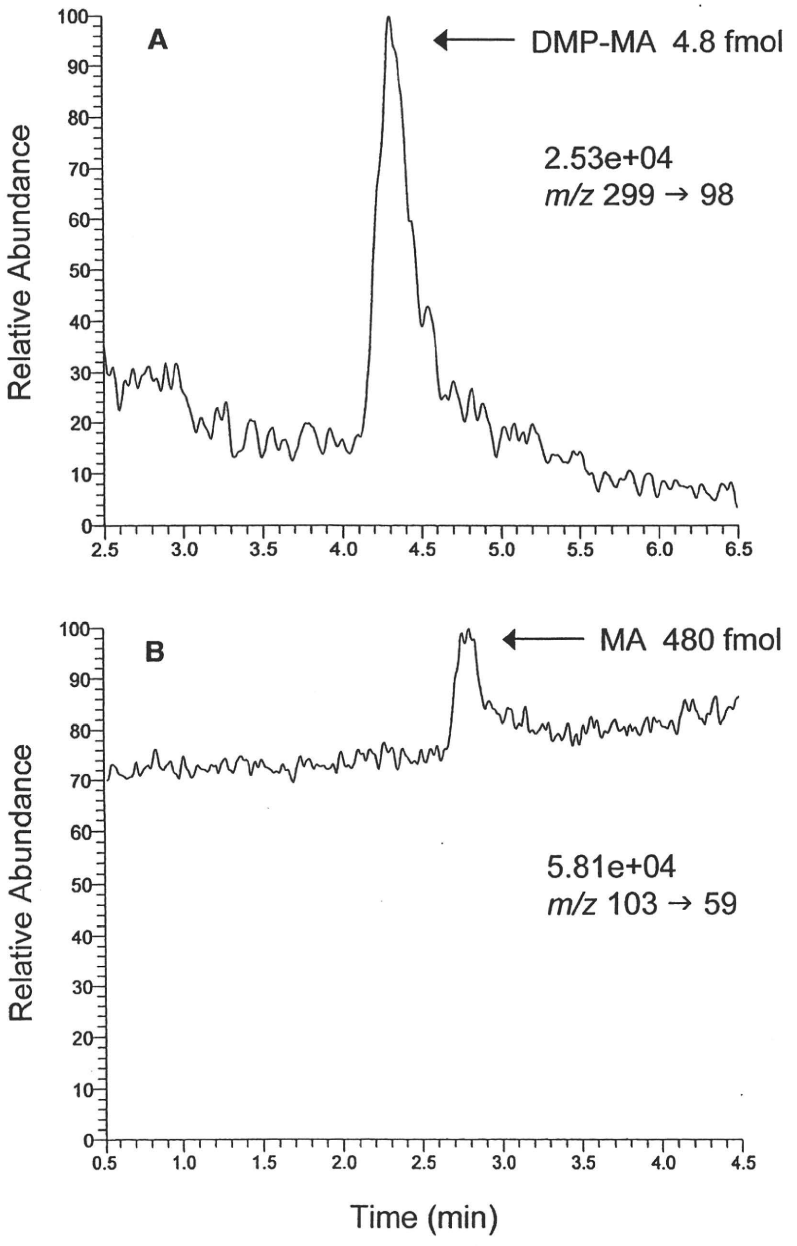

Fig. 2. Comparison of the detection limit of DMP-MA by LC-P-ESI-MS/MS at *m/z* 299 → *m/z* 98 (A) with that of MA by LC-N-ESI-MS/MS at *m/z* 103 → *m/z* 59 (B). Authentic standard of DMP-MA (4.8 fmol) or MA (480 fmol) was injected into the HPLC. The numbers written above the SRM ion pair represent the full scale of the chromatogram.

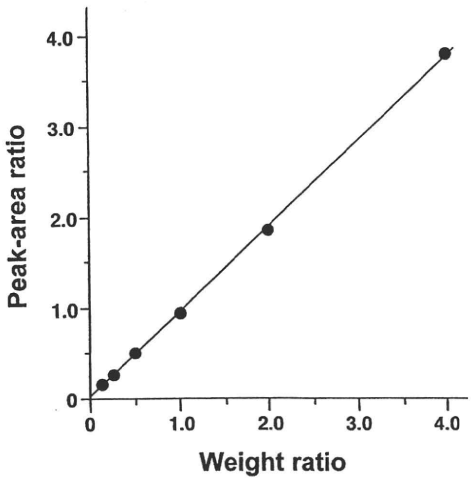

Fig. 3. Calibration curve for the weight ratio of MA to the corresponding deuterated internal standard. Linearity was checked by simple linear regression and the equation for the line of best fit was $y = 0.948x + 0.021$ ($n = 6$; $r = 1.000$; $P < 0.0001$).

but the former showed much better signal-to-noise ratio than the latter.

By N-ESI mode, authentic MA exhibited $[M-H]^-$ ion at m/z 103 as the base peak. In the MS/MS spectrum, the CH_3COO^- ion was observed at m/z 59 as the most prominent peak. The SRM was conducted using m/z 103 → m/z 59 for the MA.

Comparison of the sensitivities between P-ESI and N-ESI methods

To compare the sensitivity of DMP-MA by LC-P-ESI-MS/MS with that of MA by LC-N-ESI-MS/MS, the standard DMP-MA or MA solution was diluted and injected into the LC-MS/MS system. As shown in **Fig. 2A**, the DMP-MA was easily detected to 4.8 fmol by LC-P-ESI-MS/MS, with a signal-to-noise ratio of 10, whereas the conventional LC-N-ESI-MS/MS was barely able to detect 480 fmol of MA (Fig. 2B).

Calibration curve

A calibration curve was established for MA (**Fig. 3**). Each of different amounts (2.4, 4.8, 9.6, 19.2, 38.5, and 76.9 pmol) of authentic MA was mixed with 19.2 pmol of [$^{13}C_3$]MA, derivatized to the DMP ester and quantified as described in the Materials and Methods. The weight ratio of MA, relative to the corresponding ^{13}C-labeled internal standard, was plotted on the abscissa and the peak-area ratio of the DMP-MA to the [$^{13}C_3$] variant measured by LC-P-ESI-MS/MS was plotted on the ordinate. The linearity of the standard curve, as determined by simple linear regression, was excellent for weight ratios between 0.125 and 4.0 ($n = 6$; $r = 1.000$; $P < 0.0001$).

Representative SRM

Figure 4 shows typical SRM chromatograms for DMP-MA and the [$^{13}C_3$] variant obtained with 50 μl sera from a normal human (A) and a control rat (B). The peak-area ratio of the DMP-MA to the [$^{13}C_3$] variant was calculated from the chromatograms, and MA amount was determined by applying the ratio to the calibration curve. The peaks of DMP-MA in chromatograms A and B correspond to ~0.66 pmol (0.66 μM) and ~4.43 pmol (4.43 μM), respectively.

Precision and accuracy of the LC-P-ESI-MS/MS method

The following studies were performed to determine the precision and accuracy of the present method using the same serum obtained from a normal human subject. Reproducibility was investigated by analyzing four samples in triplicate by LC-P-ESI-MS/MS (**Table 1**). The results were analyzed by a one-way ANOVA in which the analytical errors were divided into two sources, sample preparation

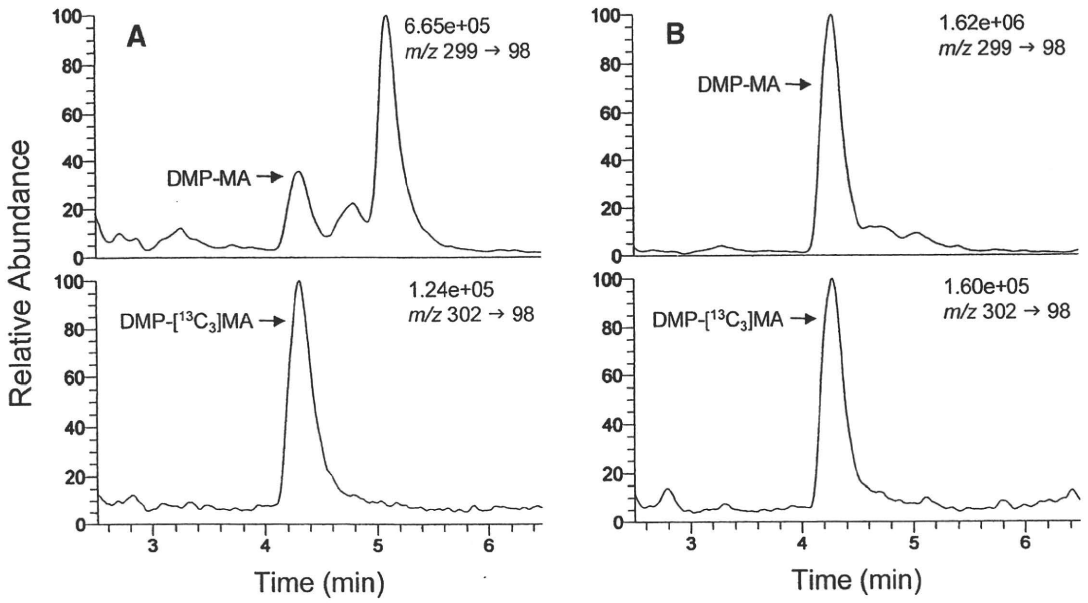

Fig. 4. Representative SRM chromatograms of DMP-MA and its $^{13}C_3$ variant (internal standard) obtained from 50 μl sera of a normal human (A) and a rat (B). The peaks of DMP-MA in chromatograms A and B correspond to ~0.66 pmol (0.66 μM) and ~4.43 pmol (4.43 μM), respectively. The numbers written above the SRM ion pair represent the full scale of the chromatogram.

TABLE 1. Reproducibility in the quantification of MA in human serum: analytical data

Sample	Individual Values			Mean ± SD
		pmol		
A	15.0	15.7	15.0	15.2 ± 0.38
B	14.4	15.6	15.5	15.2 ± 0.67
C	14.7	14.4	14.2	14.5 ± 0.29
D	15.6	15.6	14.7	15.3 ± 0.48
Mean ± SD				15.0 ± 0.58

MA was quantified in 50 μl of normal human serum.

and SRM measurement. The variances were not considered to be attributable to the sample preparation because the errors during sample preparation were not significantly larger than those between the measurements (**Table 2**). The inter-assay coefficients of variation for the between- and within-sample variations were 4.4% and 3.2%, respectively.

For the recovery experiments, known amounts of MA (a, 2a, 3a; a = 9.6 pmol) were spiked into 50 μl aliquots of the serum samples (n = 2). After the clean-up and derivatization procedures, SRM was carried out in triplicate for each sample. The recoveries of the known spiked amounts of MA ranged from 94.5% to 99.0%, with a mean of 96.0% (**Table 3**). In addition, the amount of endogenous MA found in unspiked 50 μl serum aliquots was within the 95% confidence limit for the estimated amount of MA calculated by orthogonal regression analysis, which also constituted an index for the precision and accuracy of the present method.

The circadian rhythm of MA levels in human sera

Figure 5 depicts the circadian rhythm of the serum concentrations of MA in a healthy male. Postprandial increases of MA concentrations (maximum 235% after dinner) were observed and the levels peaked between 2.5 and 6.5 h postmeal. The increase of MA concentration disappeared after skipping breakfast on the second day, which supports the idea that the diurnal pattern of serum MA concentrations is controlled mainly by food intake.

DISCUSSION

We describe a sensitive new LC-P-ESI-MS/MS method for the quantification of MA in serum. LC-N-ESI-MS/MS may be more suitable for the determination of negatively charged compounds, such as organic acids because the method does not require a derivatization step. However, as shown in Fig. 2, the sensitivity of N-ESI was not sufficient to quantify MA concentrations in a small volume of normal human serum.

Recently, we derivatized another organic acid, mevalonate, into mevalonyl-(2-pyrrolidin-1-yl-ethyl)-amide and measured it using LC-P-ESI-MS/MS (12). In this method, mevalonate was lactonized into mevalonolactone and then a tertiary amine moiety was introduced by a characteristic amidation reaction with a primary alkylamine. As a result, the tertiary amine moiety markedly promoted protonation and attomole levels of mevalonate were detected. In the present study, tertiary amine moieties were successfully introduced to MA by esterification with 3-hydroxy-1-methylpiperidine. Thus, the reaction for the synthesis of carboxylic esters by Shiina et al. (10) appears to be useful not only for the derivatization of alcohols (13) but also for that of carboxylic acids. This derivative, DMP-MA, exhibited $[M+H]^+$ as the base peak by P-ESI-MS and the detection limit by SRM was more than 100 times lower than that of underivatized MA by SRM with N-ESI mode.

The derivatization and purification steps in this method are very simple but it should be mentioned that there are two pitfalls to obtaining reliable and reproducible results. First, use of the anion exchange column cartridge gave unexpectedly high values of MA concentrations. Serum MA was extracted by this cartridge and interfering peaks on SRM chromatograms were markedly reduced by the addition of this purification step. However, the recoveries of known amounts of MA from this cartridge were always more than 100%, and additional experiments suggested that a significant amount of MA was produced from unknown substance(s) in organic solvents by this anion exchange column (data not shown). Plasma methylmalonic acid (MMA) and its isomer succinic acid (SA) are also known to be extracted by this column (14). We have derivatized MMA and SA into DMP-MMA and DMP-SA, respectively, and analyzed them by the same HPLC condition as that for DMP-MA. The SRM was conducted using m/z 313 → m/z 98 for both DMP-MMA and DMP-SA. The results showed that DMP-MMA and DMP-SA were much more hydrophobic than DMP-MA and both compounds were eluted during washout phase with 0.2% formic acid in acetonitrile (after 6 min).

Second, pH of the final sample solution should not be more than 7 because an alkaline condition easily hydrolyzes DMP-MA. After the derivatization step, most of the excess reagents and hydrophilic impurities were

TABLE 2. Reproducibility in the quantification of MA in human serum: ANOVA

Source	S	f	V	F_0	Relative SD
					%
Sample preparation	1.293	3	0.431	1.89	4.4
Error (SRM)	1.820	8	0.228		3.2
Total	3.113	11			
			$F(3,8,0.05)=4.07$		

S, residual sum of squares; f, number of degrees of freedom; f_1, $f_{\text{sample preparation}}$; f_2, f_{error}; V, unbiased variance; F_0, observed value following F distribution variance ratio ($V_{\text{sample preparation}}/V_{\text{error}}$); $F(f_1, f_2, \alpha)$, density function of F distribution with f_1 and f_2 degrees of freedom.